# MIT Libraries | DSpace@MIT

# MIT Open Access Articles

## *Grid-search event location with non-Gaussian error models*

**Massachusetts Institute of Technology**

PHYSICS
OF THE EARTH
AND PLANETARY
INTERIORS

# Grid-search event location with non-Gaussian error models[☆]

## William Rodi[*]

*Department of Earth, Atmospheric and Planetary Sciences, Massachusetts Institute of Technology,*
*77 Massachusetts Avenue, Cambridge, MA 02139, USA*

## Abstract

This study employs an event location algorithm based on grid search to investigate the possibility of improving seismic event location accuracy by using non-Gaussian error models. The primary departure from the Gaussian error model that is considered is the explicit use of non-Gaussian probability distributions in defining optimal estimates of location parameters. Specifically, the class of generalized Gaussian distributions is considered, which leads to the minimization of $L_p$ norms of arrival time residuals for arbitrary $p \geq 1$. The generalized Gaussian error models are implemented both with fixed standard errors assigned to the data and with an iterative reweighting of the data on a station/phase basis. An implicit departure from a Gaussian model is also considered, namely, the use of a simple outlier rejection criterion for disassociating arrivals during the grid-search process. These various mechanisms were applied to the ISC phase picks for the IWREF reference events, and the resulting grid-search solutions were compared to the GT locations of the events as well as the ISC solutions. The results indicate that event mislocations resulting from the minimization of $L_p$ residual norms, with $p$ near 1, are generally better than those resulting from the conventional $L_2$ norm minimization (Gaussian error assumption). However, this result did not always hold for mislocations in event depth. Further, outlier rejection and iterative reweighting, applied with $L_2$ minimization, performed nearly as well as $L_1$ minimization in some cases. The results of this study suggest that ISC can potentially improve its location capability with the use of global search methods and non-Gaussian error models. However, given the limitations of this study, further research, including the investigation of other statistical and optimization techniques not addressed here, is needed to assess this potential more completely.
©2006 Elsevier B.V. All rights reserved.

*Keywords:* Seismic event location; Grid search; ISC; ISC location workshop; IWREF data base

## 1. Introduction

The use of global optimization methods in seismic event location and other geophysical inverse problems has gained popularity in recent years as computers have become faster and the versatility of these methods has become increasingly recognized. Grid search, in particular, is a relatively simple method for event location that

deals robustly with problem non-linearity and imposes little restriction on the parameter constraints and error models that can be used (e.g. Sambridge and Kennett, 1986; Wilcock and Toomey, 1991; Dreger et al., 1998).

This study explores whether the versatility of grid-search event location can be used to produce better global earthquake locations in a routine manner. The main question addressed is whether optimality criteria based on the assumption of non-Gaussian error distributions, such as $L_1$ norm minimization, provide an automatic mechanism for mitigating the location errors induced by bad arrival time picks (outliers). Other mechanisms that are considered are an automatic association scheme, inte-

[*] Tel.: +1 617 253 7855.

*E-mail address:* rodi@mit.edu.

grated within the grid search, for rejecting outliers, and a multiple-event location scheme that simultaneously locates events and estimates an error variance for each station/phase type combination, used for reweighting the data.

The next section describes the grid-search algorithm used in this study, focusing on the above-mentioned techniques for dealing with errors in the data. The following section applies the techniques to the ISC phase picks from the 156 IWREF reference events (described in Storchak, 2006; Engdahl, 2006) and evaluates the techniques on the basis of various event mislocation statistics. The statistics are compared among the different grid-search methods and to the ISC results. The paper ends with some conclusions about whether grid search and non-Gaussian error models can be used to improve the ISC location procedures.

## 2. Event location algorithm

This study was conducted using a computer program written by the author and called GMEL, which is an acronym for "grid-search multiple event location". GMEL finds solutions to the multiple-event location problem formulated by Jordan and Sverdrup (1981), Pavlis and Booker (1983) and others, which entails finding event location and traveltime correction parameters from a set of arrival time data obtained from multiple events, stations and seismic phases. In this study, GMEL was run primarily in single-event mode, i.e. when the event locations are the only unknowns and, correspondingly, the problem decouples by events. Some runs, however, involved coupling between events and the multiple-event mode of GMEL. The following sections describe the aspects of GMEL used in this study.

### 2.1. The single-event location problem

The problem of locating a single event using $n$ seismic arrival times observed for one or more phase types at a network of stations can be expressed as:

$$d_i = T_i(\mathbf{x}) + t + e_i, \quad i = 1, \dots, n. \tag{1}$$

Here, $d_i$ is the observation for the $i$th station/phase combination; $\mathbf{x}$ and $t$ are the origin parameters (hypocenter and time, respectively) of the event; $T_i$ is a model-based traveltime function for the $i$th station/phase pair; and $e_i$ is an observational ("pick") error in $d_i$.

GMEL assumes that the pick errors are statistically independent and, following Billings et al. (1994), that each is sampled from a generalized Gaussian (or power exponential) probability distribution, whose probability

density function (p.d.f.) can be written as:

$$f[e_i] = \frac{1}{2p^{1/p}\Gamma(1 + 1/p)\sigma_i} \exp\left\{-\frac{1}{p}\left|\frac{e_i}{\sigma_i}\right|^p\right\}, \quad p \geq 1, \tag{2}$$

where $\sigma_i$ is a standard error and $\Gamma$ is Euler's gamma function. When $p = 2$, $f[\,]$ can be recognized to be a Gaussian (normal) distribution with a mean of zero and variance of $\sigma_i^2$. When $p = 1$, it is a Laplace distribution (two-sided exponential).

GMEL finds maximum-likelihood estimates of $\mathbf{x}$ and $t$, where the likelihood function is defined as the product over $i$ of the error p.d.f.s. Given the assumed form of the p.d.f.s, and assuming the $\sigma_i$ are known except for a uniform scale factor, the solutions for $\mathbf{x}$ and $t$ equivalently minimize the data misfit function given by:

$$\Psi(\mathbf{x}, t) = \sum_i \frac{1}{\sigma_i^p}|d_i - T_i(\mathbf{x}) - t|^p. \tag{3}$$

$\Psi$ is a weighted $L_p$ norm of the data residuals, raised to the power $p$. For example, an $L_2$ norm is minimized under the Gaussian error model and an $L_1$ norm is minimized under the Laplace error model.

The sum in (3) does not necessarily include all $n$ arrivals. For a given hypocenter $\mathbf{x}$, only arrivals which properly can be associated with an event at $\mathbf{x}$ are included. This excludes an arrival for which $T_i(\mathbf{x})$ is not defined (e.g. a too large epicentral distance for a Pn arrival), or an arrival whose residual is inconsistent with other residuals (an outlier). Let $A(\mathbf{x})$ denote the set of arrivals which can be associated with an event located at $\mathbf{x}$. The misfit function can then be more precisely written as:

$$\Psi(\mathbf{x}, t) = \sum_{i \in A(\mathbf{x})} \frac{1}{\sigma_i^p}|r_i(\mathbf{x}) - t|^p \tag{4}$$

where we let $r_i(\mathbf{x})$ denote the $i$th residual, given by:

$$r_i(\mathbf{x}) = d_i - T_i(\mathbf{x}). \tag{5}$$

We will denote the number of associated arrivals (the number of elements in $A(\mathbf{x})$) as $\hat{n}(\mathbf{x})$.

The optimal solution of the single-event location problem, then, is taken to be the $(\mathbf{x}, t)$ achieving the smallest $\Psi(\mathbf{x}, t)$ given that $\mathbf{x}$ achieves the highest value of $\hat{n}(\mathbf{x})$. In giving precedence to $\hat{n}$, this optimality criterion can have the effect of translating the distance and depth ranges over which the model-based traveltime functions are defined into hard constraints on the event hypocenter. While such implicit constraints can provide important information in some situations, they can potentially lead to a large event mislocation if the traveltime model poorly

predicts the distance/depth ranges of various phases or if outliers or phase misidentifications are present in the data.

### 2.2. Optimization algorithm

GMEL performs an adaptive grid search in hypocenter space to optimize $\hat{n}$ and $\Psi$ in the sense just mentioned. For each hypocenter $\mathbf{x}$ tested, the association set $A(\mathbf{x})$ is determined, and then a reduced misfit function is computed by minimizing $\Psi$ with respect to the origin time $t$:

$$\tilde{\Psi}(\mathbf{x}) = \min_t \Psi(\mathbf{x}, t) \equiv \Psi(\mathbf{x}, \hat{t}(\mathbf{x})), \tag{6}$$

where we have defined $\hat{t}$ to be the time achieving the minimum. We can find $\hat{t}$ as a solution to $\partial\Psi/\partial t = 0$, where from (4) we have:

$$\frac{\partial\Psi(\mathbf{x}, t)}{\partial t} = -p \sum_{i \in A(\mathbf{x})} \sigma_i^{-p} |r_i(\mathbf{x}) - t|^{p-2} (r_i(\mathbf{x}) - t). \tag{7}$$

For $p = 2$, the solution is simply the variance-weighted mean residual:

$$\hat{t}(\mathbf{x}) = \frac{1}{\sum_i \sigma_i^{-2}} \sum_i \sigma_i^{-2} r_i(\mathbf{x}). \tag{8}$$

In general for $p > 1$, $\partial\Psi/\partial t$ is a continuous, non-decreasing function of $t$ and a unique root can be found numerically. GMEL uses the regula falsi method for this purpose since the minimum and maximum $r_i(\mathbf{x})$ provide a convenient bracket on $\hat{t}$. Regula falsi is also used for $p = 1$, although in this case the resulting $\hat{t}$ possesses the usual non-uniqueness of a median. The value of $\tilde{\Psi}(\mathbf{x})$ is well-defined nonetheless.

The grid-search algorithm itself is a recursive scheme that tests hypocenters that are nodes on successively finer grids. The search grids are defined in a spherical system whose independent coordinates are depth and the epicentral distance and azimuth from a specified reference point. The grids are truncated by a maximum epicentral distance and by upper and lower bounds on depth, all specified in advance.

The search logic borrows key elements from the neighborhood algorithm of Sambridge (1999). On a given pass of the search, a list of the best hypocenters found thus far are retained, and new contenders are added to the list as local neighbors of these. The local neighbors of a hypocenter are chosen systematically, rather than randomly, as adjacent points in one of the search coordinates (selected alternately) at a refined grid spacing. For example, if the current depth grid spacing is $h$ and a hypocenter with depth $z$ is chosen for refinement

in depth, then the added neighbors have the same epicenter and depths $z \pm h/3$. After calculating $\hat{n}$ and $\tilde{\Psi}$ for the added contenders, a test is performed to determine which hypocenters will be retained for the next pass of the search. The criterion is that the reduced misfit function be closer to the smallest value ($\tilde{\Psi}_{\text{best}}$) than the largest value ($\tilde{\Psi}_{\text{worst}}$) achieved by the hypocenters on the current search list (considering only those having the largest association set). That is, the hypocenter $\mathbf{x}$ is retained, and will contribute new neighbors, if:

$$\tilde{\Psi}(\mathbf{x}) \leq \frac{\tilde{\Psi}_{\text{worst}} + \tilde{\Psi}_{\text{best}}}{2}. \tag{9}$$

In addition, a ceiling is imposed on the number of hypocenters that have a common ascendant from which they were refined. This forces the search to be even more global than the retention criterion alone. The grid search is stopped when the grid spacing in all three coordinates reaches a specified hypocenter resolution.

### 2.3. Outlier rejection (association)

GMEL allows the use of an outlier criterion in determining the associate set, $A(\mathbf{x})$, in addition to the requirement that the model-based traveltime be defined. When evaluating a test hypocenter $\mathbf{x}$, each arrival is assigned a time window, $w_i$, defined by:

$$w_i(\mathbf{x}) = \frac{\delta\Delta}{\Delta_i(\mathbf{x})} T_i(\mathbf{x}) + \tau_i(\mathbf{x}). \tag{10}$$

$\delta\Delta$ is the current search grid spacing in the epicentral direction, while $\Delta_i(\mathbf{x})$ is the epicentral distance between $\mathbf{x}$ and the station for arrival $i$. $\tau_i$ is the 0.001 point on the error probability distribution for arrival $i$: $f_i[\tau_i] = 0.001 f_i[0]$, where $f_i[\,]$ is the generalized Gaussian distribution in (2). The $i$th arrival is associated with an event at $\mathbf{x}$ if its residual is within $w_i$ of the weighted mean residual. We can write this criterion as (omitting the $\mathbf{x}$ dependence):

$$\bar{r} - w_i \leq r_i \leq \bar{r} + w_i, \tag{11}$$

where

$$\bar{r} = \frac{1}{\sum_{i \in A} w_i^{-1}} \sum_{i \in A} w_i^{-1} r_i, \tag{12}$$

$A$ being an initial association set. Arrivals that fail this criterion are removed from $A$, for the hypocenter $\mathbf{x}$ under evaluation.

It is important to note that this association scheme is embedded in the grid-search algorithm, rather than applied only to an initial location for the event. That is, the association set is determined separately for each

hypocenter tested in the search. However, numerical experiments indicated that the scheme is effective only if, after determining the associated arrivals, a follow-up grid search is performed with the association set fixed. This may reflect a pitfall of giving precedence to maximizing the size of the association set in the optimality criterion.

### 2.4. Reweighting data by station/phase pairs

This technique brings in one aspect of the multiple-event location problem, which we describe briefly. Let us use $j$ as an event index and write, for example, the hypocenter of the $j$th event as $\mathbf{x}_j$ and the arrival time of the $i$th station/phase pair from the $j$th event (if it was observed) as $d_{ij}$. Reweighting the data for a station/phase pair means that its standard error, $\sigma_i$, is estimated from the set of residuals for that pair. Fixing the location parameters for the events to current estimates, the maximum-likelihood estimate of $\sigma_i$ is given by:

$$\hat{\sigma}_i = \left( \frac{1}{n_i} \sum_j |d_{ij} - T_i(\hat{\mathbf{x}}_j) - \hat{\imath}_j|^p \right)^{1/p} \tag{13}$$

where $n_i$ is the number of arrivals associated with some event. GMEL clips this estimate to obey prior bounds on the relative values of the $\hat{\sigma}_i$. The bounds can be expressed as:

$$\beta_{min} \leq \frac{\hat{\sigma}_i}{v_i} \leq \beta_{max}, \tag{14}$$

where $\beta_{min}$ and $\beta_{max}$ are specified, and the $v_i$ are nominal standard errors, whose relative values are fixed but whose absolute values are scaled so that the grand residual norm, summed over all events, stations and phases, equals the total number of data.

The estimation of the $\sigma_i$ couples the location problem across events. Therefore, when station/phase reweighting is enabled, GMEL performs single-event location iteratively. After locating each of the events on a given pass of the iteration, the $\hat{\sigma}_i$ are computed using Eqs. (13) and (14) and these values are used as the standard errors in the next pass of event location, which updates the $(\hat{\mathbf{x}}_j, \hat{\imath}_j)$. The iteration stops when the $\hat{\sigma}_i$ converge.

### 2.5. Comparison to ISC procedures

In the terms defined here, the event location algorithm used at ISC performs single-event location using an iterative, gradient-based search procedure (Adams et al., 1982). With fixed data weights ($\sigma_i$), the algorithm would correspond to the Gauss–Newton method

(Geiger's method) and would minimize the data misfit function, $\Psi$, implied by a Gaussian error model ($p = 2$). However, a significant departure of the ISC algorithm from the Gauss–Newton method is its use of Jeffreys' method of uniform reduction (Jeffreys, 1932) to reweight the data at each step of the iteration. The reweighting increases the standard error $\sigma_i$ for larger residuals $r_i$, which has the effect of desensitizing the location solution to data outliers. The method of uniform reduction implicitly generalizes the probability model for pick errors to be non-Gaussian but it can introduce additional challenges for a gradient-based search method, such as dependence of the location solution on the initial hypocenter seed (Buland, 1986).

The ISC location algorithm does not perform automatic outlier rejection as part of the iterative solution process, although some data rejection criteria are applied a priori (D. Storchak, private communication). However, the ISC algorithm does re-identify phase types automatically, which GMEL does not do.

## 3. Application to the IWREF data base

### 3.1. Overview

This section considers the accuracy of GMEL and ISC solutions for the IWREF reference event list, described by Storchak (2006) and Engdahl (2006). The mislocation errors in GMEL solutions, obtained in various ways, are compared to the ISC mislocations and to each other. The ISC solutions are actually of two types: ones determined with the location procedures used prior to 2001, and ones determined with improved procedures established in 2001. In this paper, we will refer to these as ISC1 and ISC2 solutions, respectively. There are ISC1 solutions for 152 of the 156 IWREF events and ISC2 solutions for all 156 events. The ISC2 solutions were computed recently by reprocessing the archived picks (D. Storchak, private communication).

GMEL solutions for the IWREF events were obtained in the following ways:

(1) The error distribution was varied between Gaussian ($L_2$ norm minimization) and Laplace ($L_1$ norm minimization). Five values of the parameter $p$ (in Eq. (2)) were tested: $p = 2$, 1.75, 1.5, 1.25 and 1.
(2) Solutions were obtained with (a) outlier rejection invoked, (b) station/phase data reweighting invoked, and (c) neither. Outlier rejection and reweighting were not used simultaneously.
(3) The phase picks used to locate the events were either (a) the set of ISC1-defining phases, (b) the set

Table 1
Number of arrivals in three ISC data sets for the IWREF events

| Phase | Data set | | |
|---|---|---|---|
| | ISC1 | ISC2 | ISC3 |
| P | 34289 | 34118 | 34555 |
| Pn | 3557 | 3543 | 3563 |
| Pb | 262 | 286 | 288 |
| Pg | 274 | 531 | 535 |
| S | 0 | 2903 | 4808 |
| Sn | 0 | 893 | 954 |
| Sb | 0 | 138 | 145 |
| Sg | 0 | 250 | 256 |
| Pdiff | 0 | 0 | 446 |
| PKPdf | 0 | 0 | 2634 |
| PKPbc | 0 | 0 | 135 |
| PKPab | 0 | 0 | 128 |
| Sdiff | 0 | 0 | 9 |
| SKSac | 0 | 0 | 6 |
| Total | 38382 | 42662 | 48462 |

of ISC2-defining phases, or (c) all direct P and S arrivals (whether used by ISC or not).

With regard to item (3), the phases defining the ISC1 solutions for the 152-event subset comprised only direct teleseismic and regional P arrivals, most (89%) being teleseismic P. None of the arrivals was a surface reflection, core phase or the Pdiff phase. The ISC2-defining phases comprised, additionally, direct teleseismic and regional S arrivals. The third data set considered, which we will label ISC3 here, includes all direct P and S arrivals, whether or not they were defining phases for the ISC locations. The main additions in ISC3 are core transmitted and diffracted phases. Table 1 gives the arrival counts by phase type for each data set.

The GMEL solutions were obtained with nominal standard errors ($v_i$ in (14)) set to 1.0 s for P phases and 2.0 s for S phases. Traveltimes were modeled by interpolating traveltime tables generated for the AK135 Earth model. Weak location constraints were used in the grid searches to ensure minimal effect on the solutions: epicenters were constrained to be within 500 km of the ISC solution and, for free-depth solutions, focal depth was bounded between 0 and 250 km. Only a few event locations, obtained with the ISC3 data set, were affected by these constraints.

GMEL uses an assigned traveltime table for each phase type, as identified on input, and does not attempt to re-identify phases when inconsistencies between the tables and observed arrival times occur. The following steps were taken in this study to accommodate this limitation:

(1) The forward model for GMEL used "composite" traveltime tables for certain phase types. Specifically, phases labeled P or Pdiff were modeled with a first-arrival P table (earliest of all direct P phases); Pb was modeled as the earlier of Pg and Pb; and Pn arrivals were modeled as the earliest of Pg, Pb and Pn. A specific table was used for each PKP branch. Analogous composite and specific tables were used for S phases.
(2) Arrivals identified as simply PKP or SKS, with no branch specified, were not used. This affected only the ISC3 data set.
(3) An arrival was excluded if its calculated traveltime, using the AK135 tables and ISC location, was not defined. This criterion eliminated 13 arrivals from the ISC2 data set and 228 arrivals from the ISC3 data set.

The composite traveltime tables were inconsistent with a small portion of the data, e.g. when a station reported Pb and Pn for the same event. The arrivals eliminated by steps (2) and (3) are not included in the Table 1 counts.

The comparisons below report various mislocation statistics for the event epicenters and depths. The statistics are calculated from the absolute difference between a solution location (ISC or GMEL) and the IWREF ground-truth location. For depths, the difference is simply the absolute value $|\hat{z} - z^{GT}|$. For epicenters, the absolute mislocation is the great-circle distance between the solution and GT epicenter. The statistics reported are the median (50‰), 75‰ and 90‰ points among the mislocations for the event set under consideration. Maximum mislocations are also reported for some of the cases.

The grid searches performed in these examples were run with very conservative search parameters so that numerical precision did not affect the performance of the various techniques. However, some additional runs with the ISC2 data set indicated that the grid-search algorithm tested roughly 1000 hypocenters (per event, with depth free) to achieve a hypocentral precision of 0.1 km.

### 3.2. Comparison of GMEL and ISC solutions

To compare GMEL and ISC solutions for the IWREF event locations, GMEL was run using the arrival times only for the defining phases of the ISC locations (summarized in Table 1). Additionally, when ISC fixed the depth of an event to a default value, GMEL constrained the depth of that event to the same value. ISC uses default depths for known chemical or nuclear explosions and when focal depth is poorly constrained by the data.
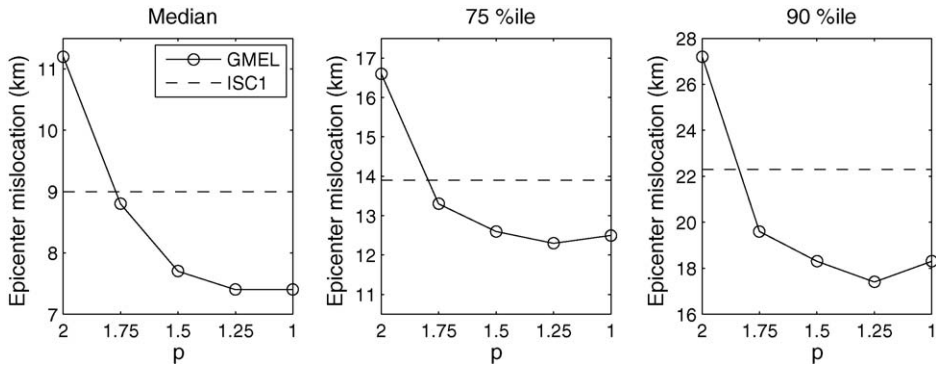
Fig. 1. Mislocation statistics for ISC and GMEL solutions for 88 IWREF event epicenters, obtained using a fixed-depth constraint and the ISC1 defining phase set (all direct P waves). The GMEL solutions are shown for five values of $p$, the order of the residual norm that was minimized.

In the ISC1 solutions, 88 of the 152 IWREF events were assigned default depths. Ninety-one out of 156 ISC2 solutions have default depths. All the GMEL solutions discussed in this section were obtained without using the outlier rejection and data reweighting techniques described in Sections 2.3 and 2.4.

Fig. 1 compares the epicenter mislocation statistics for the 88 fixed-depth ISC1 and GMEL solutions, obtained with the ISC1 defining phases. GMEL solutions are shown as a function of the error-distribution parameter $p$. The results tell a very simple story: location accuracy is significantly better for smaller values of $p$, with the $p = 2$ GMEL mislocations being worse than the ISC1 mislocations and the $p < 2$ GMEL mislocations being better. The story for the 64 free-depth solutions, Fig. 2, is less clear-cut. The GMEL epicenter mislocations are generally better with smaller $p$, but none of the GMEL cases is better than the ISC1 result. The GMEL depth mislocation statistics (bottom panels) are worse than the ISC1 ones, and do not improve with smaller $p$ (the 75‰ is actually worst for $p = 1$). These differences in performance may not be significant considering that
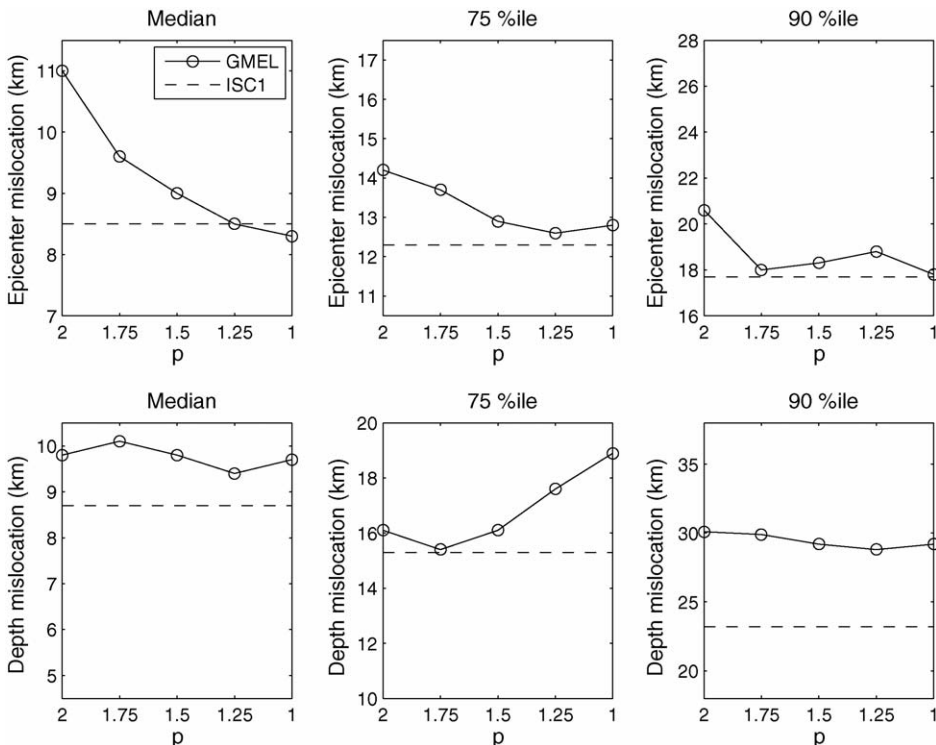


Fig. 2. Mislocation statistics for ISC and GMEL free-depth solutions for 64 IWREF event locations, obtained using the ISC1 defining phase set.
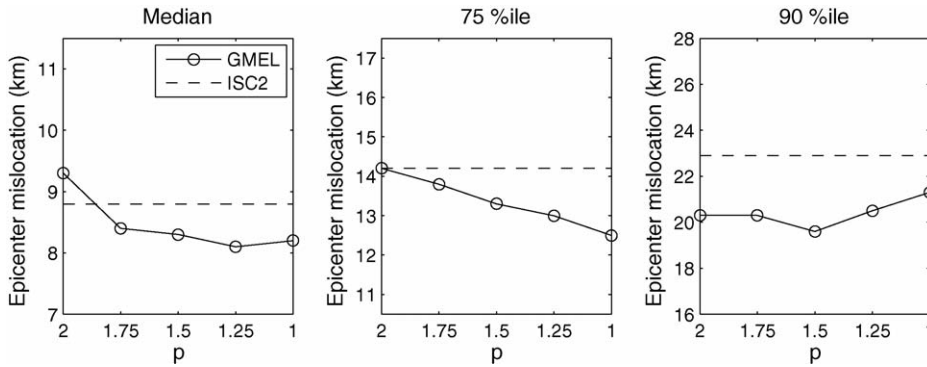
Fig. 3. Mislocation statistics for ISC and GMEL fixed-depth solutions for 91 IWREF event locations, obtained using the ISC2 defining phase set.

the GT depths may have errors up to 5 km. However, the unexpected dependence of the depth mislocations on $p$ suggests the possibility that depth solutions are less susceptible to outliers when depth control is poor, as it is with direct P wave arrivals alone.

The analogous mislocation results obtained by using the ISC2 defining phases are shown in Figs. 3 and 4. For the 91 fixed-depth events, the GMEL epicenter mislocations for $p < 2$ are modestly smaller than the ISC2 mislocations. For the 65 free-depth events, the GMEL epicenter mislocations (top panels of Fig. 4) are generally not as good as the ISC2 counterparts but are nearly

so for small $p$. The GMEL depth mislocations (bottom panels) show the same reverse dependence on $p$ as before, but it is noteworthy that they are significantly better than both the ISC2 depth mislocations and the GMEL depth mislocations resulting from the ISC1 data set. One can infer that the addition of S wave arrivals, while only about 10% of the ISC2 data set, has improved the control on the focal depth for at least some of these events.

Lastly, Fig. 5 shows the largest mislocations (100‰) resulting from the ISC and GMEL solutions, obtained with both the ISC1 and ISC2 data sets. The relative performance of the ISC and GMEL solutions, and the de-
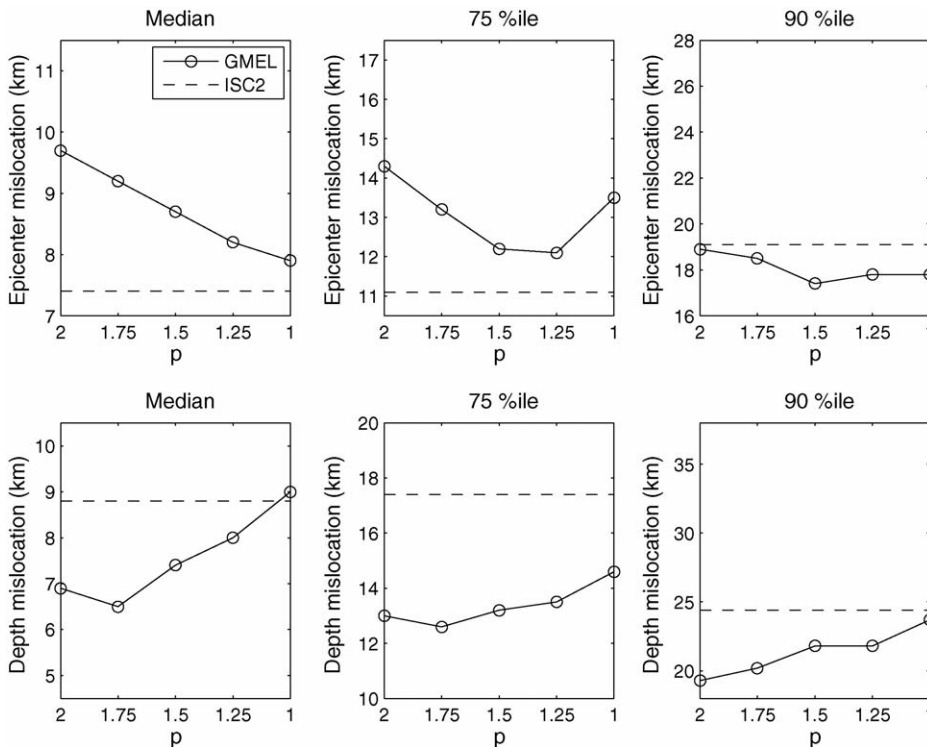


Fig. 4. Mislocation statistics for ISC and GMEL free-depth solutions for 65 IWREF event locations, obtained using the ISC2 defining phase set.
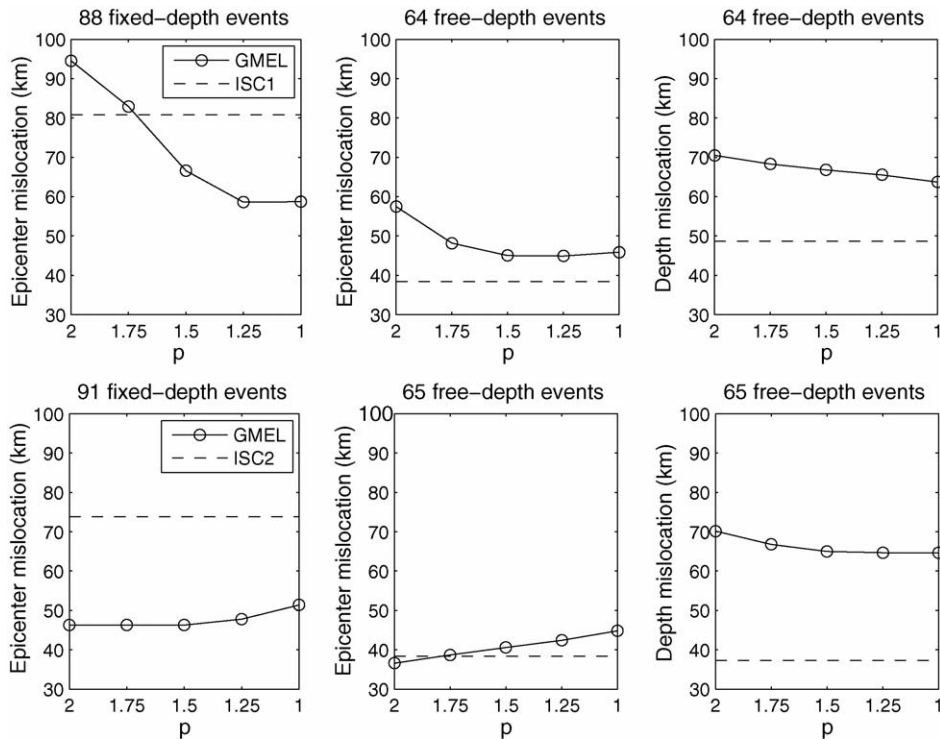
Fig. 5. Maximum mislocations for the ISC and GMEL fixed- and free-depth solutions obtained with the ISC1 defining phases (top panels) and ISC2 defining phases (bottom panels).

pendence of the latter on $p$, are qualitatively similar to the results for the other mislocation statistics (previous four figures). The most noticeable differences are for the solutions obtained with the ISC2 defining phases (bottom panels of Fig. 5), where the maximum epicenter mislocation among the fixed-depth events is much smaller for the GMEL solutions than the ISC2 solution (lower left panel), and the maximum depth mislocation among the free-depth events is much larger for the GMEL solutions (lower right).

### 3.3. Comparison of $L_p$ norms, outlier rejection and date reweighting

This section considers only GMEL solutions for the IWREF event locations, and compares the performance of different mechanisms for desensitizing location estimates to outliers. All the solutions allowed the focal depth to be free for all of the events, bounded between 0 and 250 km. Solutions were found using the three data sets described in Section 3.1.

The outlier rejection technique was described in Section 2.3. Table 2 shows the number of unassociated arrivals that resulted for each GMEL solution that used this feature. The fewest arrivals were rejected from the ISC2

data set, which comprised the defining phases for the reprocessed ISC locations. For the ISC1 and ISC3 data sets, the rejected data included many arrivals with apparent timing errors of 1 min or, in the case of ISC3, several minutes up to 1 h. The table also shows that, for each data set, the number of unassociated phases decreases as $p$ decreases, reflecting the decreasing sensitivity of $L_p$ norms to large residuals. Comparing Tables 1 and 2 one can infer that the number of ISC3 arrivals that were associated (not rejected) exceeds the full ISC2 data by 4500–4800 arrivals, showing that most of the 5800 additional phases in ISC3 became defining phases in the GMEL solutions.

Table 2
Number of unassociated arrivals resulting when outlier rejection is used

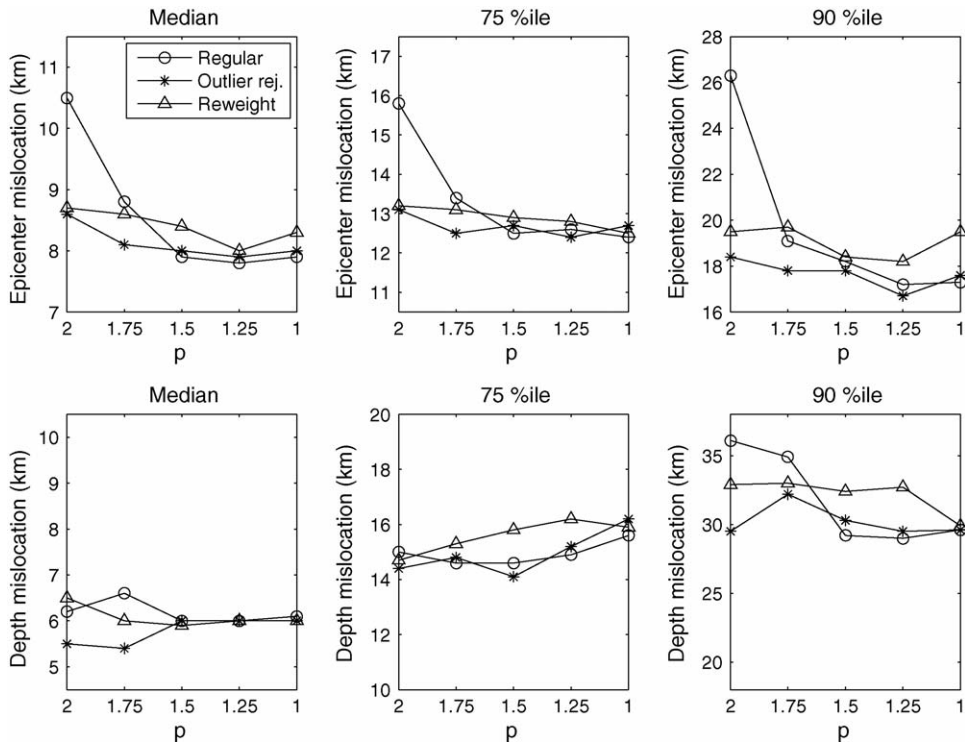| $p$ | Data set | | |
|---|---|---|---|
| | ISC1 | ISC2 | ISC3 |
| 2 | 795 | 721 | 1310 |
| 1.75 | 771 | 607 | 1218 |
| 1.5 | 725 | 498 | 1215 |
| 1.25 | 620 | 448 | 1066 |
| 1 | 605 | 381 | 995 |

Fig. 6. Mislocation statistics for GMEL solutions for 152 IWREF event locations, obtained with the defining phases for the ISC1 solutions. Focal depth was unconstrained (free) for all 152 events. The results labeled "regular" were obtained without either outlier rejection ("outlier rej.") or data reweighting ("reweight").

The iterative reweighting scheme used by GMEL was described in Section 2.4. When reweighting was not used, the relative standard errors were fixed between arrivals, in the ratio of 1:2 between P and S wave arrivals (as in the last section). When reweighting was used, the relative standard errors were allowed to vary within bounds defined by Eq. (14), with $\beta_{min}$ and $\beta_{max}$ set to 0.5 and 2, respectively. This implies that standard errors among P arrivals could vary by a factor of 4, and the same for S arrivals. The relative P:S standard errors could vary between 2:1 and 1:8.

Fig. 6 shows the mislocation results for the ISC1 data set. When outlier rejection and data reweighting are not used ("regular") we see that the epicenter mislocation statistics (top panels) improve with decreasing $p$, as they did earlier when most of the events had fixed depths. We can also see that the solutions obtained with outlier rejection and data reweighting for $p = 2$ are almost as good as the "regular" $p = 1$ solution. Not surprisingly, all the $p = 1$ solutions display similar performance. The situation with the depth mislocations is different (bottom panels). The results do not depend systematically on $p$ and, while outlier rejection outperformed reweighting,

neither yielded a major improvement to the regular $p = 2$ solution.

The results for the ISC2 data set are shown in Fig. 7. With this data set, which includes S phases, data reweighting improves the $L_2$ epicenter mislocations significantly, matching the regular $L_1$ performance. Outlier rejection had little effect with the ISC2 data set, which probably owes to the fact that this data set is not corrupted with large timing errors.

The most dramatic differences among methods occur when they are applied to the ISC3 data set, which includes direct arrivals not used in the ISC solutions. These results are shown in Fig. 8. First, we can see that both the epicenter and depth mislocations for the regular $p = 2$ solution are much worse than in the ISC1 and ISC2 cases (note some altered vertical scales). The mislocations for the regular case improve significantly with decreasing $p$. Data reweighting and, especially, outlier rejection also improve the $p = 2$ mislocations significantly, with outlier rejection at $p = 2$ being comparable to the $L_1$ results. Comparing to the previous figure, the $L_1$ mislocation statistics for the ISC3 data set are similar to those for the ISC2 data set.
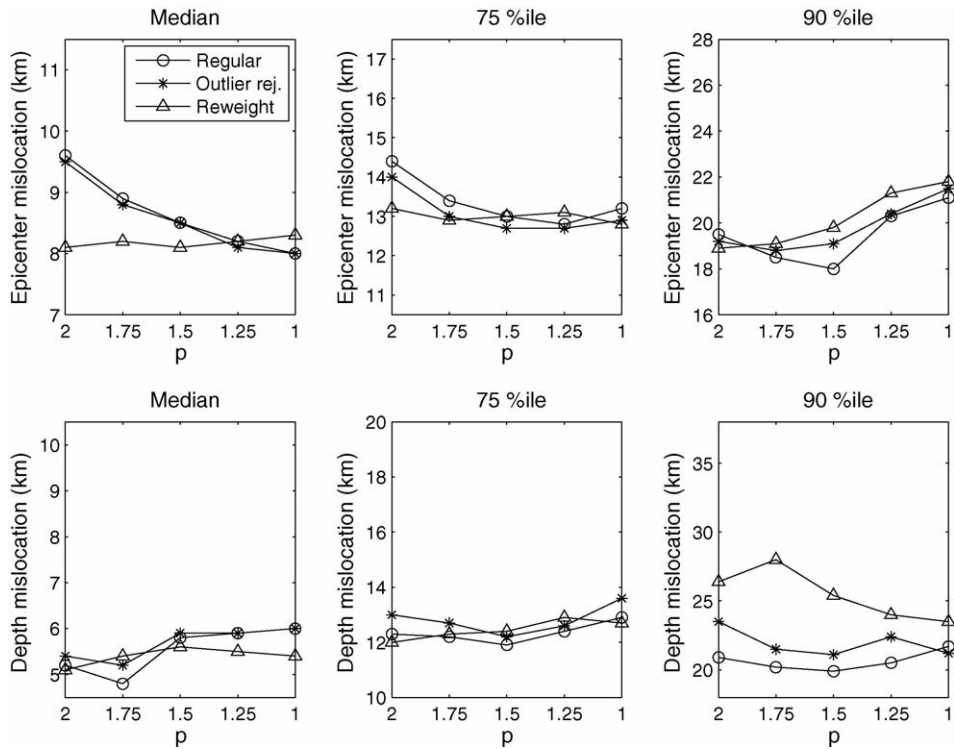
Fig. 7. Mislocation statistics for GMEL free-depth solutions for 156 IWREF event locations, obtained with the ISC2 defining phases.
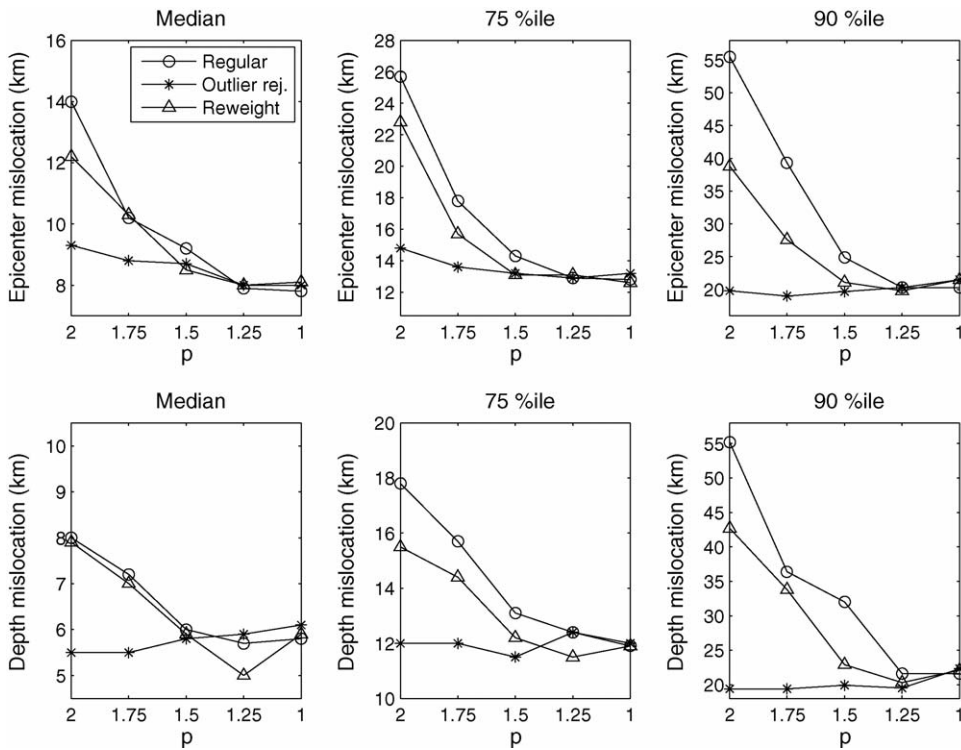


Fig. 8. Mislocation statistics for GMEL free-depth solutions for 156 IWREF event locations, obtained with the ISC3 data set, i.e. defining and non-defining direct P and S arrivals.

## 4. Discussion and conclusions

The experiments with grid-search event location presented here indicate that, overall, $L_p$ norm minimization with values of $p$ close to 1 yields better location accuracy than the conventional practice of $L_2$ norm minimization. An $L_1$ norm, to highlight the limiting case, is less sensitive to large residuals and its use in a misfit criterion effects an implicit mechanism for rejecting outlier arrival time picks. In the maximum likelihood context, the decreased sensitivity to outliers arises from the long tails of the Laplace probability distribution.

Comparing to the ISC solutions for the IWREF events, the grid-search solutions obtained with small $p$ generally had smaller epicenter mislocations than the ISC solutions but did not consistently improve depth mislocations. The improvement in epicenter mislocations was most apparent with the original "ISC1" data set, which contained many defining phases with very large residuals. This suggests indirectly that $L_1$ (or $L_{<1.5}$) minimization may work at least as well as the method of uniform reduction, used in the ISC location algorithm, as a way to automatically desensitize location estimates to outliers. The original ISC solutions for earthquake depths, however, were better than the grid-search results, which actually showed little dependence on $p$ or even reverse dependence, i.e. best for $p = 2$. An explanation may be that pick errors and outliers are a less important issue than data coverage in the case of focal depth estimation with data sets dominated by teleseismic P arrivals. This explanation is consistent with the results of the last experiment shown (Fig. 8), where smaller $p$ did yield smaller depth mislocations when using the larger (ISC3) data set that includes more phase types and more poor quality picks.

The embedding of outlier rejection in the grid search, and iterative reweighting of the data for each station/phase combination, both improved the $L_2$ minimization criterion and, in some cases, performed as well as or slightly better than the $L_1$ criterion. The greatest performance difference between these alternatives occurred with the full set of direct arrivals, where outlier rejection with $p = 2$ did significantly better than data reweighting and almost as well as $L_1$ minimization.

The techniques investigated here were only tested in limited versions, e.g. with one choice of bounds on the data weights and one criterion for identifying outliers. Moreover, the tests revealed some limitations of the grid-search algorithm used. In particular, its optimality criterion, which gives priority to maximizing the number of defining phases, may be vulnerable to outliers and contentious with automatic outlier removal. Further, the algorithm does not re-identify phases, requiring misidentified phases to be rejected as outliers.

While these experiments were too limited to predict which non-Gaussian error approach would work best in routine application, there is clear suggestion that $L_p$ minimization, with $p$ near 1, may accomplish more simply and reliably the goals of automatic data rejection and reweighting schemes. However, some experiments indicated that simple rejection and reweighting schemes may have a valuable role when data sets contain secondary or low signal-to-noise arrivals, which can be difficult to identify and pick. This and other studies (e.g. Kennett, 2006) demonstrate the flexibility of global search methods for implementing non-Gaussian techniques in a rigorous way. The main recommendation of this study, therefore, is that ISC adopt a global-search event location algorithm as a platform for further research on the performance of new optimization criteria and statistical techniques in routine event location.

## References

Adams, R.D., Hughes, A.A., McGregor, D.M., 1982. Analysis procedures at the International Seismological Centre. Phys. Earth Planet. Interiors 30, 85–93.

Billings, S.D., Sambridge, M.S., Kennett, B.L.N., 1994. Errors in hypocenter location: picking, model and magnitude dependence. Bull. Seismol. Soc. Am. 84, 1978–1990.

Buland, R., 1986. Uniform reduction error analysis. Bull. Seismol. Soc. Am. 76, 217–230.

Dreger, D., Uhrhammer, R., Pasyanos, M., Franck, J., Romanowicz, B., 1998. Regional and far-regional earthquake locations and source parameters using sparse broadband networks: a test on the Ridgecrest sequence. Bull. Seismol. Soc. Am. 88, 1353–1362.

Engdahl, E.R., 2006. Application of an improved algorithm to high precision relocation of ISC test events. Phys. Earth Planet. Interiors. 158, 14–18.

Jeffreys, H., 1932. An alternative to the rejection of observations. Proc. Roy. Soc. Lond. 187, 78–87.

Jordan, T.H., Sverdrup, K.A., 1981. Teleseismic location techniques and their application to earthquake clusters in the south-central Pacific. Bull. Seismol. Soc. Am. 71, 1105–1130.

Kennett, B.L.N., 2006. Non-linear methods for event location in a global context. Phys. Earth Planet. Interiors. 158, 46–54.

Pavlis, G.L., Booker, J.R., 1983. Progressive multiple event location (PMEL). Bull. Seismol. Soc. Am. 73, 1753–1777.

Sambridge, M., 1999. Geophysical inversion with a neighbourhood algorithm. I. Searching a parameter space. Geophys. J. Int. 138, 479–494.

Sambridge, M.S., Kennett, B.L.N., 1986. A novel method of hypocentre location. Geophys. J. Roy. Astr. Soc. 87, 679–697.

Storchak, D.A., 2006. Results of locating the IASPEI GT(0–5) reference events using the standard ISC procedures. Phys. Earth Planet. Interiors. 158, 4–13.

Wilcock, W.S.D., Toomey, D.R., 1991. Estimating hypocentral uncertainties for marine microearthquake surveys: a comparison of the generalized inverse and grid search methods. Mar. Geophys. Res. 13, 161–171.